arXiv:1109.0247v1 [cond-mat.stat-mech] 1 Sep 2011

Phys. Rev. E 84, 031102 (2011)

Glassy phases and driven response of the phase-field-crystal model with random pinning

E. Granato [1,2], J.A.P. Ramos [1,3], C.V. Achim [4,5], J. Lehikoinen [4], S.C. Ying [2], T. Ala-Nissila [2,4], and K.R. Elder [6]

[1] *Laboratório Associado de Sensores e Materiais, Instituto Nacional de Pesquisas Espaciais,12227-010 São José dos Campos, SP, Brazil*

[2] *Department of Physics, P.O. Box 1843, Brown University, Providence, RI 02912-1843, USA*

[3] *Departamento de Ciências Exatas, Universidade Estadual do Sudoeste da Bahia, 45000-000 Vitória da Conquista, BA,Brazil*

[4] *Department of Applied Physics, Aalto University School of Science, P.O. Box 11000, FI-00076 Aalto, Espoo, Finland*

[5] *Institut für Theoretische Physik II: Weiche Materie, Heinrich-Heine-Universität Düsseldorf, Universitätsstraße 1, D-40225 Düsseldorf, Germany and*

[6] *Department of Physics, Oakland University, Rochester, Michigan 48309-4487, USA*

We study the structural correlations and the nonlinear response to a driving force of a two-dimensional phase-field-crystal model with random pinning. The model provides an effective continuous description of lattice systems in the presence of disordered external pinning centers, allowing for both elastic and plastic deformations. We find that the phase-field crystal with disorder assumes an amorphous glassy ground state, with only short-ranged positional and orientational correlations even in the limit of weak disorder. Under increasing driving force, the pinned amorphous-glass phase evolves into a moving plastic-flow phase and then finally a moving smectic phase. The transverse response of the moving smectic phase shows a vanishing transverse critical force for increasing system sizes.

PACS numbers: 64.60.Cn, 68.43.De

I. INTRODUCTION

Pinning and sliding of lattice systems, which can form periodic structures in the absence of perturbations, are subjects of considerable interest. In the presence of pinning disorder and driving forces, they can exhibit a wide variety of interesting equilibrium and non-equilibrium behavior with partially ordered and glassy structures. Important examples in two dimensions include vortex lattices in superconducting films [1], atomic layers adsorbed between sliding surfaces [2] or on oscillating substrates [3, 4], and colloidal crystals on a rough substrate [5, 6]. Although in three dimensions a topological ordered phase, the Bragg glass [7], with quasi-long range positional order is possible in the weak disorder regime, the two-dimensional limit is qualitatively different due to the proliferation of thermally and disorder-induced dislocations even in the weak-disorder regime. Analytical and numerical studies for the equilibrium behavior [7–12] have shown that, in two dimensions, positional and orientational order are both destroyed by weak pinning disorder and topological defects at any nonzero temperature leading to a liquid-like phase in the thermodynamic limit. In the absence of thermal fluctuations (zero temperature) an amorphous glass is expected [9, 13]. For the system under a driving force moving at high velocities, it has been shown analytically that some components of the disorder remain static in the co-moving reference frame, leading to a moving glass phase [13]. In three-dimensional systems, such state can show topological order as a moving Bragg glass [13–15]. In two dimensions, however, this phase corresponds to a moving smectic glass, which retains quasi long-range order in the direction transverse to the driving force but only exponential correlations in the parallel direction [13, 14, 16–21].

In modeling such lattice systems, both for static and dynamic properties, it is essential to include the periodicity of the lattice and allow for topological defects (dislocations and disclinations). These topological defects are not contained in pure elastic models that have completely different properties, specially in two dimensions. A phase-field-crystal (PFC) model was introduced recently [22–24] that allows for both elastic deformations and topological defects within an effective continuous description of the lattice system while still retaining information on short length scales. By extending the PFC model to take into account the effect of an external periodic pinning potential [25], a two-dimensional version of the model has been used to describe commensurate-incommensurate transitions in the presence of thermal fluctuations [26] and the driven response [27] including inertial effects [28]. However, in order to study the statics and dynamics of the disordered system, quenched pinning disorder needs to be included in the PFC modeling.

In this work, we study the structural correlations and nonlinear response to a driving force of a two-dimensional PFC model with random pinning. The model provides an effective continuous description of lattice systems in presence of disordered external pinning centers, allowing for both elastic and plastic deformations. We show that in the presence of disorder, the phase-field crystal assume an amorphous glassy ground state, with only short-ranged positional and orientational correlations even in

the limit of weak disorder. Under increasing driving force, the pinned amorphous-glass phase evolves into a moving plastic-flow phase and then finally a smectic phase. The transverse response of the moving smectic phase shows a vanishing transverse critical force for increasing system sizes.

II. PFC MODEL WITH RANDOM PINNING POTENTIAL

The effective Hamiltonian of the PFC model with an external pinning potential [25] can be written in a dimensionless form as

$$H_{\rm pfc} = \int d\vec{x}\{\frac{1}{2}\psi[r+(1+\nabla^2)^2]\psi+\frac{\psi^4}{4}+V(\vec{x})\psi(\vec{x})\}, \quad (1)$$

where $\psi(\vec{x})$ is a continuous field at position $\vec{x}$ in two dimensions and $V(\vec{x})$ is the pinning potential. The field $\psi(\vec{x})$ is conserved and its average value, $\bar{\psi}$, together with r are the relevant parameters in the model.

In the absence of the pinning potential, $V(\vec{x}) = 0$, the energy functional of Eq. (1) can be minimized by a configuration of the field $\psi(\vec{x})$ forming a hexagonal pattern of peaks with wave vector of magnitude $|\vec{Q}| \approx 1$, when the values of the parameters r and $\bar{\psi}$ are chosen appropriately. This structure of peaks can be regarded as the ground state of a lattice system with perfect crystalline order, where the phase field $\psi(\vec{x})$ represents the deviation of the particle number density $\rho(\vec{x})$ from a reference value ρ_0, $\psi(\vec{x}) = (\rho(\vec{x})-\rho_0)/\rho_0$. The energy functional of Eq. (1) can then be used to describe both elastic as well plastic properties of the lattice system [22, 23], including the effects of thermal fluctuations [26]. An external driving force $\vec{f}$ in the lattice system, can be represented by an additional contribution to the effective Hamiltonian as

$$H_f = -\int d\vec{x}\rho(\vec{x})\vec{x}\cdot\vec{f}, \quad (2)$$

which will lead to nonequilibrium behavior. The effects of the driving force have been recently investigated in some detail [27, 28], in absence of disorder. Inertial effects of the lattice system can also be described within the PFC model, by including an additional kinetic energy contribution to the effective Hamiltonian as

$$H_{kin} = \int d\vec{x}\frac{\vec{g}^2(\vec{x})}{2\rho(\vec{x})}, \quad (3)$$

where $\vec{g}(\vec{x})$ is the momentum density field.

The dynamical equations describing the time evolution of the lattice system in presence of thermal fluctuations and the external force can be written as [28]

$$\frac{\partial\psi}{\partial t} = -\nabla\cdot\vec{g}; \quad (4)$$

$$\begin{aligned}\frac{\partial g_i}{\partial t} &= -\nabla_i\frac{\delta H_{\rm pfc}}{\delta\psi} \;+\; \psi f_i - \gamma g_i + \nu_i(\vec{x},t);\\ \langle\nu_i(\vec{x},t)\nu_j(\vec{x}',t')\rangle &= 2k_BT\gamma\delta(\vec{x}-\vec{x}')\delta(t-t')\delta_{i,j},\end{aligned}$$

where $\vec{f} = (f_x, f_y)$ is the spatially uniform external force and $\vec{\nu}(\vec{x},t)$ is a thermal noise satisfying the fluctuation-dissipation relation corresponding to a temperature T and damping coefficient γ.

In the present work, we only consider the limit of very large γ, when inertial effects are negligible, leading to the overdamped dynamical equations

$$\begin{aligned}\frac{\partial\psi(\vec{x},t)}{\partial t} &= -\nabla\cdot\vec{g}; \quad (5)\\ \gamma g_i &= -\nabla_i\frac{\delta H_{\rm pfc}}{\delta\psi} \;+\; \psi(\vec{x},t) f_i + \nu_i(\vec{x},t);\\ \langle\nu_i(\vec{x},t)\nu_j(\vec{x}',t')\rangle &= 2k_BT\gamma\delta(\vec{x}-\vec{x}')\delta(t-t')\delta_{i,j},\end{aligned}$$

The above coupled equations for ψ and $\vec{g}$ can also be combined into a single equation for ψ, giving

$$\begin{aligned}\gamma\frac{\partial\psi}{\partial t} &= \nabla^2\frac{\delta H_{\rm pfc}}{\delta\psi} \;-\; \vec{f}\cdot\nabla\psi + \zeta(\vec{x},t); \quad (6)\\ \langle\zeta(\vec{x},t)\zeta(\vec{x}',t')\rangle &= 2k_BT\gamma\nabla^2\delta(\vec{x}-\vec{x}')\delta(t-t').\end{aligned}$$

The generalization of the PFC model with an external periodic pinning potential studied previously [25–28] to the case of a quenched random pinning potential considered here is straightforward. Such a model is relevant for studying diverse systems such as, adsorbate layers with quenched impurities or on substrates with disorder, and vortex lattice in superconductors in the presence of pinning centers. To this end we model the quenched potential in the simplest way by defining at every spatial location $V(\vec{x}) = D\mu(\vec{x})$, where $\mu(\vec{x})$ is a δ-correlated distribution

$$\langle\mu(\vec{x})\mu(\vec{x}')\rangle = \delta(\vec{x}-\vec{x}'), \quad (7)$$

and D is an amplitude characterizing the strength of the disorder. Since, there is no characteristic length scale in such pinning potential, it is particularly suitable for the investigation of finite-size effects using small system sizes as done in this work. In this *dense* pinning model, the separation between pinning centers can be much smaller than the distance between the density peaks in the phase-field crystal. This corresponds to a physical system where the length scale of the varying pinning potential is smaller than the average lattice spacing of the system. Such a scenario could be realized *e.g.* in the case of colloidal particles confined near a rough glass plate [5, 6].

For the numerical calculations, the phase field $\psi(\vec{x})$ is defined on a space grid (idx, jdy) with periodic boundary conditions. The simulations in presence of thermal fluctuations and the driving force were performed using Eq. (5), using Euler's method with the Laplacians and gradients evaluated by finite differences. In the absence of external force and thermal fluctuations, the equation of

motion (6) was used in most simulations, and solved using a semi-implicit algorithm. The linear part is treated implicitly, while the non-linear term is treated explicitly [29]. The field at time $t + dt$ is obtained according to

$$\hat{\psi}(\vec{k}, t + dt) = \frac{\hat{\psi}(\vec{k}, t) + (-k^2)\hat{NT}(\vec{k}, t)}{1 - dt(-k^2)\hat{\omega}(\vec{k})}, \tag{8}$$

where, $\hat{\psi}(\vec{k}, t)$ is the Fourier transform of $\psi(\vec{r}, t)$, $-k^2$ is the equivalent in inverse space of the laplacian ∇^2 and $\omega(\vec{k}) = r + (1 - k^2)^2$ is the inverse space equivalent of the linear operator $r + (1 + \nabla^2)^2$. The term $\hat{NT}(\vec{k}, t)$ is the Fourier transform of the nonlinear part $\psi(\vec{x}, t)^3 + V(\vec{x})$.

III. POSITIONAL AND ORIENTATIONAL CORRELATIONS

To investigate the influence of disorder on the structural properties of the phase-field crystal, we study the behavior of the static correlation functions from calculations of the structure factor $S(\vec{k})$ and orientational susceptibility χ, which measure translational order and orientational order [30], respectively. $S(\vec{k})$ can be obtained from the positions $\vec{R}_j$ of the peaks in the phase-field pattern as

$$S(\vec{k}) = \frac{1}{N_p} \sum_{j,j'=1}^{N_P} e^{-i\vec{k}\cdot(\vec{R}_j - \vec{R}_{j'})}, \tag{9}$$

where N_p is the number of peaks, while χ can be obtained from the local orientational order parameter $\phi_6(R_j)$ as

$$\chi = \frac{1}{N_p} \sum_{j,j'=1}^{N_p} \phi_6(R_j)\phi_6^*(R_{j'}). \tag{10}$$

The orientational order parameter $\phi_6(R_j)$ is a measure of the six-fold orientational symmetry of the crystalline order and is defined as

$$\phi_6(R_j) = \frac{1}{N_j} \sum_{l=1}^{N_j} e^{i6\theta_{j,l}}, \tag{11}$$

where the summation is taken over the N_j nearest neighbors of the peak at position $\vec{R}_j$ and $\theta_{j,l}$ is the angle of the bond jl with an arbitrary axis. The disorder averaged $S(k)$ and χ are obtained by averaging over different realizations of the disorder configurations $V(\vec{x})$.

In the absence of disorder, solutions of the PFC model form a periodic hexagonal array of peaks in the ground state with wavevector $\vec{Q}$, which has both long range positional and six-fold orientational order. Positional order can be characterized by the scaling of the structure factor $S(Q)$ with system size L, which behaves as $S(Q) \propto L^2$ for a perfectly ordered state. Disorder can destroy positional long range order and lead to quasi long-range or short-range positional order, which corresponds to correlations that decay with distance r as a power law $r^{-\eta}$ or exponentially $e^{-r/\xi}$, respectively. For these distinct types of correlations the corresponding structure factor is expected to behave as $S(Q) \propto L^{2-\eta}$ and $S(Q) \propto const.$, for large system sizes. We find it convenient to define an *effective exponent* η_p to characterized the positional order in different regimes, from a power law fit of the normalized structure peak as

$$S(Q)/N_p \propto L^{-\eta_p}. \tag{12}$$

With this definition, since $N_p \propto L^2$, $\eta_p \to 0$ indicates long range order, $\eta_p \to \eta < 2$ quasi long-range order and $\eta_p \to 2$ short-range order. An analogous effective exponent η_o characterizing the orientational correlations, can be defined from the finite-size dependence of the orientational susceptibility χ as

$$\chi/N_p \propto L^{-\eta_o}. \tag{13}$$

IV. NUMERICAL RESULTS AND DISCUSSION

In this section, we present our numerical results for the static behavior and the driven response of the phase-field crystal at zero temperature (without thermal noise), obtained in the absence and presence of the external force, respectively. The dynamical equations, Eqs. (5) and (6), were integrated numerically on a uniform square grid with $dy = dx = \pi/4$. The total system size $L_x dx \times L_y dy$ accommodates approximately $L^2/100$ density maxima. The PFC parameters are set to $r = \bar{\psi} = -1/4$, where the ground state of the model is a perfectly ordered hexagonal phase in the absence of disorder, and $\gamma = 1$. For the case without external force and thermal fluctuations we used a rectangular box of size $L_x dx \times L_y dy$ with $dy = \pi/4$ and $dx = dy/(\sqrt{(3)}/2)$. In order to check the size effect we performed calculations for several values of L_x from 128 to 512.

A. Ground state

We first search for the the lowest-energy state of the phase-field crystal in the absence of the external driving force. For this purpose, we have used the simulated annealing method to avoid trapping in higher energy metastable states. First, simulations of equilibrium states at some initial temperature corresponding to finite noise terms in the dynamical equation (Eq. (5)) are performed using arbitrary initial configurations. Then the initial temperature is slowly decreased to zero leading to a final configuration with a minimum energy. This annealing procedure is repeated for different initial configurations and the zero-temperature configuration with the lowest energy is identified as the ground state.

Fig. 1 shows the behavior of the structure factor peak and orientational susceptibility as function of the system

size obtained by simulated annealing, in the weak disorder regime, $D = 0.03$. The effective exponent for both positional and orientational correlations obtained from a power law fit of the size dependence in Fig. 1 is consistent with two, indicating that correlations are short ranged. Larger disorder strength gives the same result. This behavior suggests that the ground state of the phase-field crystal in presence of pinning disorder is an amorphous glass. This is expected on theoretical grounds. In fact, analytical studies by renormalization-group methods [7–9] and computer simulations [10, 12] indicate that, in two dimensions, quasi long-range positional and orientational order are destroyed by weak disorder or thermal fluctuations, leading to a liquid-like phase in the thermodynamic limit. In the absence of thermal fluctuations (zero temperature) an amorphous-glass state is expected [9, 13]. The length scale for the crossover to such state increases with decreasing disorder strength.

Long-range order in presence of weak disorder has been found at low temperatures in some other models [31], which however describe structural (internal) disorder [9, 32] rather than external pinning disorder as considered here. On the other hand, in some molecular-dynamics simulations of particle models of colloidal crystals on a disordered substrate [33], quasi long-range order was observed at low temperatures in a weak disorder regime, although no detailed finite-size analysis was carried out. Quasi long-range order has also been observed in experiments on colloidal crystals on a rough substrate [6]. However, the apparent positional and orientational order in such cases can also be explained as a finite-size effect due to a large but finite crossover length scale, which increases with decreasing disorder strength [9, 11]. Another possible explanation is the effect of slow dynamics, which requires a much longer time scale to observe the true equilibrium state, leading to partially-ordered metastable states. In Sec. IVc, we examine similar states for the PFC model, which were obtained using the dynamical equations in absence of thermal annealing.

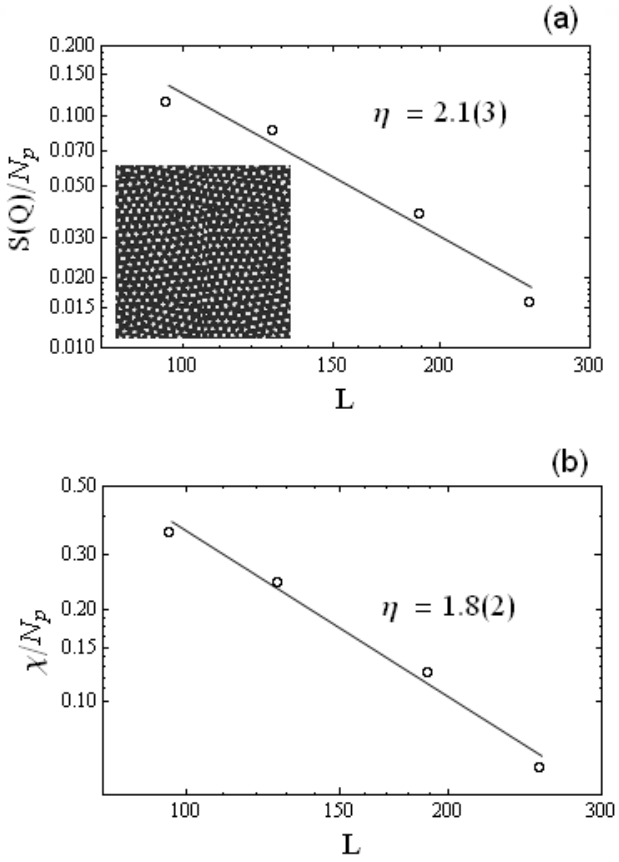


FIG. 1: Size dependence of the (a) structure factor peak and (b) orientational susceptibility, for weak disorder $D = 0.03$, obtained from simulated annealing. The straight lines are power-law fits to the data, $S(Q)/N_p \propto L^{-\eta_p}$ and $\chi/N_p \propto L^{-\eta_o}$. Inset in (a): lowest-energy pattern of the phase field $\psi(\vec{x})$ for $L = 190$.

B. Behavior under a driving force

To obtain the driven response of solutions of the phase-field crystal model, we determine the steady state velocity of the peaks under a constant external force as described by Eq. (5). The velocity is measured by tracking the position of the peaks $\vec{R}_i(t)$ in the phase field $\psi(\vec{x})$ during the simulation [27]. From the velocities of the peak positions $\vec{v}_i = d\vec{R}_i/dt$, the steady state drift velocity is obtained as

$$\vec{v} = \langle \frac{1}{N_P} \sum_{i=1}^{N_P} \vec{v}_i(t) \rangle, \tag{14}$$

where N_P is the number of peaks and $\langle ... \rangle$ denotes time average. The disorder averaged drift velocity is then obtained by averaging over different realizations of the disorder configurations. The calculations were done without thermal noise (zero temperature). The initial state at $f = 0$ is obtained from simulated annealing as described in Sec. IVa. The velocity response of the phase-field crystal to the applied driving force is shown Fig. 2 for strong disorder $D = 0.1$. The velocity response is nonlinear, with different behavior at low and large driving forces, due to the effects of pinning. This property is observed in different lattice systems with quenched disorder [13, 14, 34]. At sufficiently low drive, the drift velocity is negligibly small and the phase-field crystal remains pinned in the amorphous glassy phase. As the force increases beyond a critical value, $f_c \approx 0.05$, corresponding to a depinning transition, the phase-field crystal moves with increasing steady-state velocity but with different patterns at low and high velocities as can be seen from the corresponding configurations in Fig. 3. At low velocities above the critical force f_c, the pattern of the phase field has a liquid-like structure as shown in Fig. 3a for $f = 0.2$. The trajectories of the local maxima in the phase field $\psi(\vec{x})$ correspond to a plastic flow due to

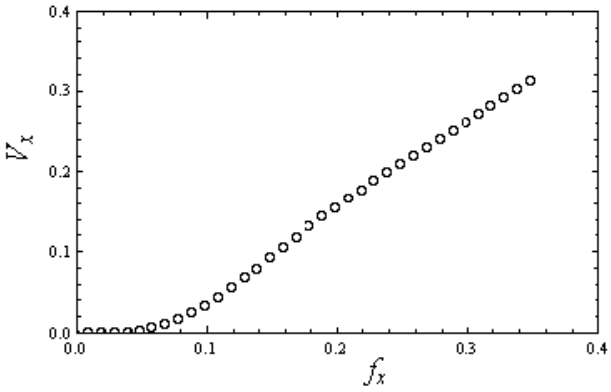


FIG. 2: Longitudinal velocity response V_x to a driving force f_x averaged over disorder, for $D = 0.1$ and $L = 128$.

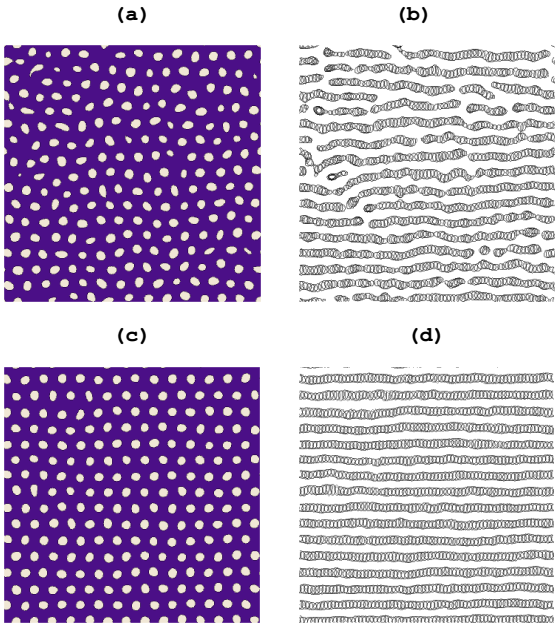


FIG. 3: (Color online) Snapshot of the phase field $\psi(\vec{x})$ and corresponding trajectories of the peaks in $\psi(\vec{x})$ in the moving state. (a) and (b) for $f = 0.2$ and (c) and (d) for $f = 0.8$. Results are for $L = 128$ and $D = 0.1$. The trajectories in (b) and (d)) are superpositions of snapshots of the peaks (open circles in (a) and (c)) at consecutive times.

pinned and unpinned regions. For this moving state, the corresponding structure factor (Fig. 4), averaged over time and disorder, shows small and broad peaks. For larger values of the driving force above a characteristic value f_d, there is a dynamical reordering transition to a moving partially ordered phase as shown in Fig. 3c for $f = 0.8$. The trajectories of the local maxima form well defined static channels parallel to the driving force. The structure factor now become larger and sharper as shown in Fig. 4. Rough estimates of critical values f_c and f_d obtained for different disorder strengths were used to construct the qualitative dynamical phase diagram as a function of disorder strength and applied force shown in Fig. 5.

The nature of the moving phase at high velocities is particularly interesting. Since the pinning potential acts as a time oscillating perturbation in the co-moving reference frame, one would expects that the disorder effects on the initial hexagonal structure should decrease with increasing velocity. However, it has been shown that some components of the disorder remain static [13], leading to a moving glass phase. In two dimensions, such a phase corresponds to a moving transverse glass characterized by a smectic-like structure, which retains quasi long-range order in the direction perpendicular to the applied force but only exponential correlations in the direction parallel to the force [13, 14]. This moving smectic state has been observed in many different driven systems with disorder [16–21]. Indeed, for the present driven PFC model, the pattern for the large driving force in Fig. 3d also shows a smectic-like structure. To verify this behavior more quantitatively, we have studied the finite-size dependence of the structure factor peaks (Fig. 4) in the transverse and longitudinal directions for the sliding state at $f = 0.8$. The results shown in a log-log plot in Fig. 6 are consistent with a smectic phase in the thermodynamic limit, where ordering only occurs in one spatial direction. The height of the peaks in the transverse direction decreases slowly with system size as a power law $S/N_P^2 \propto L^{-\eta}$ with $\eta \approx 0.3(1)$, consistent with quasi long-range order, while in the longitudinal direction it decreases much faster with $\eta \approx 1.4(6)$ as expected for short-range order. This estimate of the critical exponent η for the transverse peaks in the driven phase-field crystal is comparable to the result, $\eta = 0.5(1)$, obtained for a particle model of driven vortex lattices in disordered superconductors [16].

Another important property of the moving glass state at large velocities is the existence of barriers to transverse motion. It was predicted [13] that this should lead to a transverse critical force at zero temperature for an additional external force applied perpendicular to the initially driving force. However, it has also been argued [14] that the transverse response at zero temperature is nonuniversal, and qualitatively different behavior is possible for different physical systems. The former scenario of transverse depinning has already been observed for driven vortex lattices [16–21]. To find out which scenario is realized in the present version of the PFC model, we have studied the velocity response in the transverse direction V_y at a large longitudinal force f_x for different realizations of the disorder configurations. We find that the transverse depinning force is very sensitive to the dis-

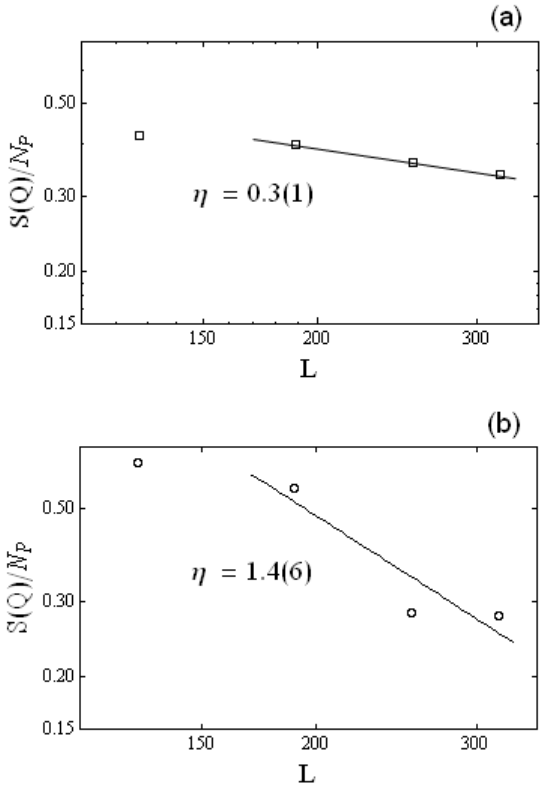


FIG. 6: Finite-size behavior of the (a) transverse and (b) longitudinal peaks in the structure factor, for the moving state at $f_x = 0.8$. The straight lines are power-law fits to the data, $S(Q)/N_p \propto L^{-\eta}$, for the largest sizes.

FIG. 4: Structure factor, averaged of the disorder, in the moving state, for (a) $f = 0.2$ and (b) $f = 0.8$. Results are for $L = 128$ and $D = 0.1$.

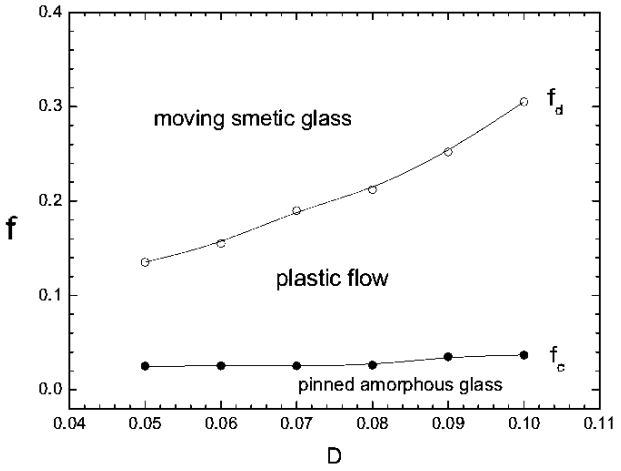


FIG. 5: Qualitative dynamical phase diagram as a function of disorder strength D and applied force f. f_c is the depinning force and f_d is the critical value for the transition from plastic flow to moving glass regimes.

order configurations and seems to vanish in some cases as can be seen in Fig. 7, where the transverse velocity response is shown for different realizations of the disorder configuration for a system size $L = 128$. To investigate if the transverse critical force is still nonzero in the large system limit, we performed calculations for increasing system sizes and the results were averaged over different disorder configurations. Fig. 8 shows that the critical value f_{cy} for the onset of transverse depinning decreases with increasing system size and therefore may actually vanish in the thermodynamic limit. Although such behavior is possible according to analytical arguments [14], it is unclear at the present which distinct feature of the PFC model is responsible for it. Since a transverse critical force has been found for the same model in the case of periodic pinning [27], we can only speculate that the presence of disorder allows some defects to be generated even by small transverse forces.

C. Glassy metastable states

In the previous section IVa we have determined the lowest energy state in absence of a driving force (ground

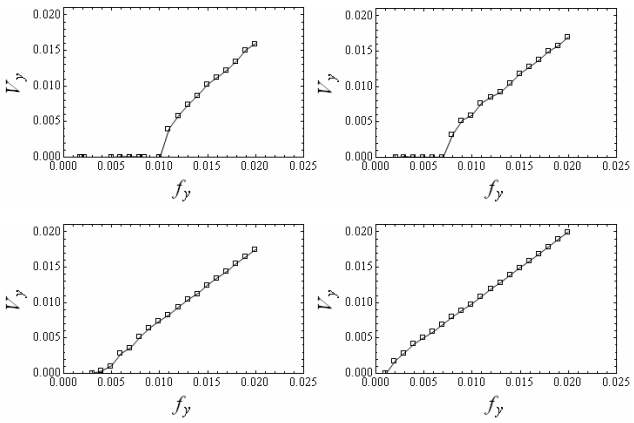


FIG. 7: Transverse velocity response V_y to an additional force f_y for different disorder configurations, for the moving state at $f_x = 0.8$ when $D = 0.1$ and $L = 128$.

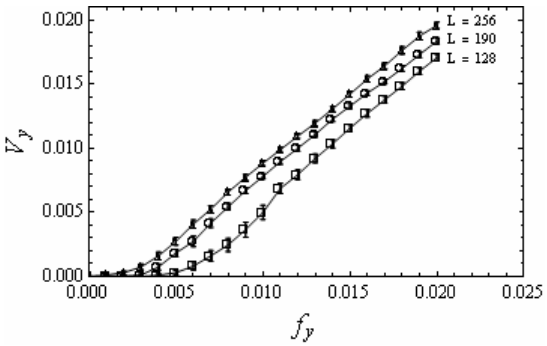


FIG. 8: Finite-size dependence of the transverse velocity response V_y to an additional force f_y averaged over disorder, for the moving state at $f_x = 0.8$ and $D = 0.1$.

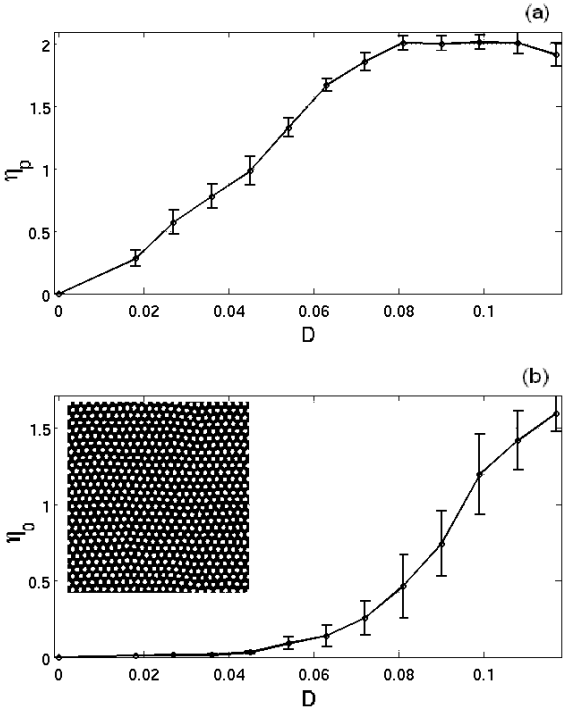


FIG. 9: Effective power-law exponents for (a) positional η_p and (b) orientational η_o correlation functions, obtained from the dynamical equations without thermal noise. Inset in (b): phase field pattern for $D = 0.036$.

state) using simulated annealing methods and found that the configuration corresponds to an amorphous glass state, with only short-ranged positional and orientational correlations. In this section, we will discuss some metastable states. These are states corresponding to local minima rather than the global minimum for the ground state. Nonetheless, they may still be relevant under suitable experimental conditions.

Metastable states were obtained by starting with the perfect hexagonal ground state in the absence of disorder and then allowing the system to evolve according to the dynamical equation for a relatively short period $(5 \times 10^5 dt, dt = 0.5\ )$, for different disorder strengths in the absence of thermal noise. The disorder strength D is incremented in steps of 0.009.

Fig. 9 shows the behavior of the effective exponents η_p and η_o for positional and orientational correlations of the final static configuration as a function of the disorder strength D. It appears that there are three different thresholds values of D: $D_1 \approx 0.04$, $D_2 \approx 0.08$ and $D_3 >> 0.12$. Below D_1, the *weak-disorder* regime, the system has long-range orientational order and quasi-long range translational order. Between D_1 and D_2 the system exhibits both quasi-long range orientational and translation order. Between D_2 and D_3 a hexatic ordering occurs which corresponds to quasi-long range orientational order and short-range translational order. This phase ordering is analogous to such a phase that occurs in two dimensional crystals induced by thermal flucuations [30]. Finally above D_3, which is beyond the range of D investigated, we expect that only short-range orientational and translational order should remain. As described in Sec. IVa, the lowest-energy state obtained by simulated annealing is an amorphous glass rather than a partially-ordered state observed in such netastable states. In fact, the Inset in Fig. 9 indicates that the phase-field crystal would remain essentially ordered for weak pinning if no simulated annealing was performed. However, even in this weak disorder regime correlations are actually short ranged if the system is allowed to reach its true ground state, as can be seen from the Inset in Fig. 1. Although the ground state is an amorphous glass, the thresholds D_1 D_2 and D_3 in Fig. 9 can represent some characteristic values for non-equilibrium behavior.

We have also investigated the metastable states for a different model of disorder. In this *sparse* pinning model, the pinning sites are separated by a minimum distance $L_p \approx 2\pi/(|\vec{Q}|\sqrt{(3)}/2))$, *i.e.* they cannot come closer to each other than the particles in the ideal hexagonal

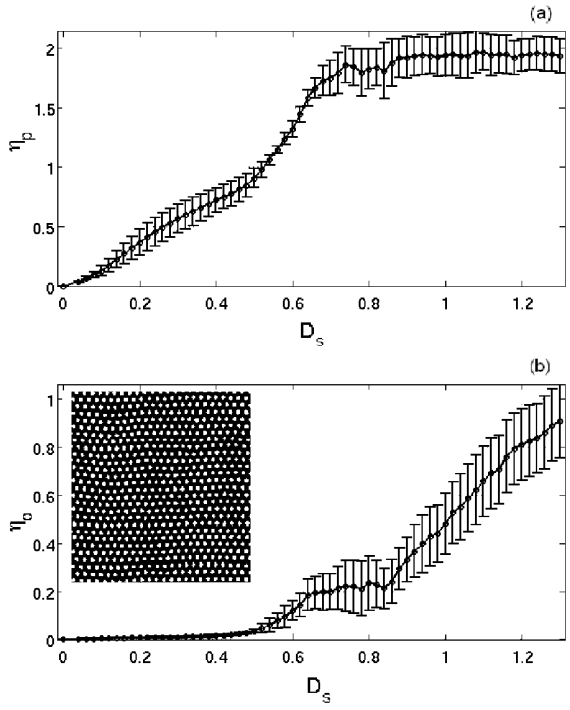


FIG. 10: Effective power-law exponents for (a) positional η_p and (b) orientational η_o correlation functions in the *sparse* pinning model (see text for details), obtained from the dynamical equations without thermal noise. Inset in (b): phase field pattern for $D_s = 0.4$.

ground state of the PFC model with wave vector $\vec{Q}$. Such model may be realized *e.g.* in the case of adsorbed atomic layers on a substrate with impurities [2]. A finite density ρ_s of randomly distributed pinning centers is assigned with pinning strength (amplitude) D_s. Thus, unlike the *dense* pinning model discussed above, there are now two relevant parameters, namely ρ_s and D_s. Metastable states were obtained again starting from the hexagonal state and incrementing D_s in steps of 0.02, while the density of pinning sites ρ_s was fixed to $\rho_s = 0.0082$. For this density of the pinning centers the ratio between the pinning centers and the number of maxima of the ideal triangular lattice is 0.375. Fig. 10 shows the behavior of the effective exponents η_p and η_o for positional and orientational correlations of the final static configuration as a function of the disorder strength D_s obtained in this sparse disorder model. Although the errorbars are relatively large, there is again three distinct thresholds values, $D_1 \approx 0.45$, $D_2 \approx 0.7$ and presumably $D_3 >> 1.3$. The results are qualitatively the same as that for the dense pinning model.

V. CONCLUSIONS

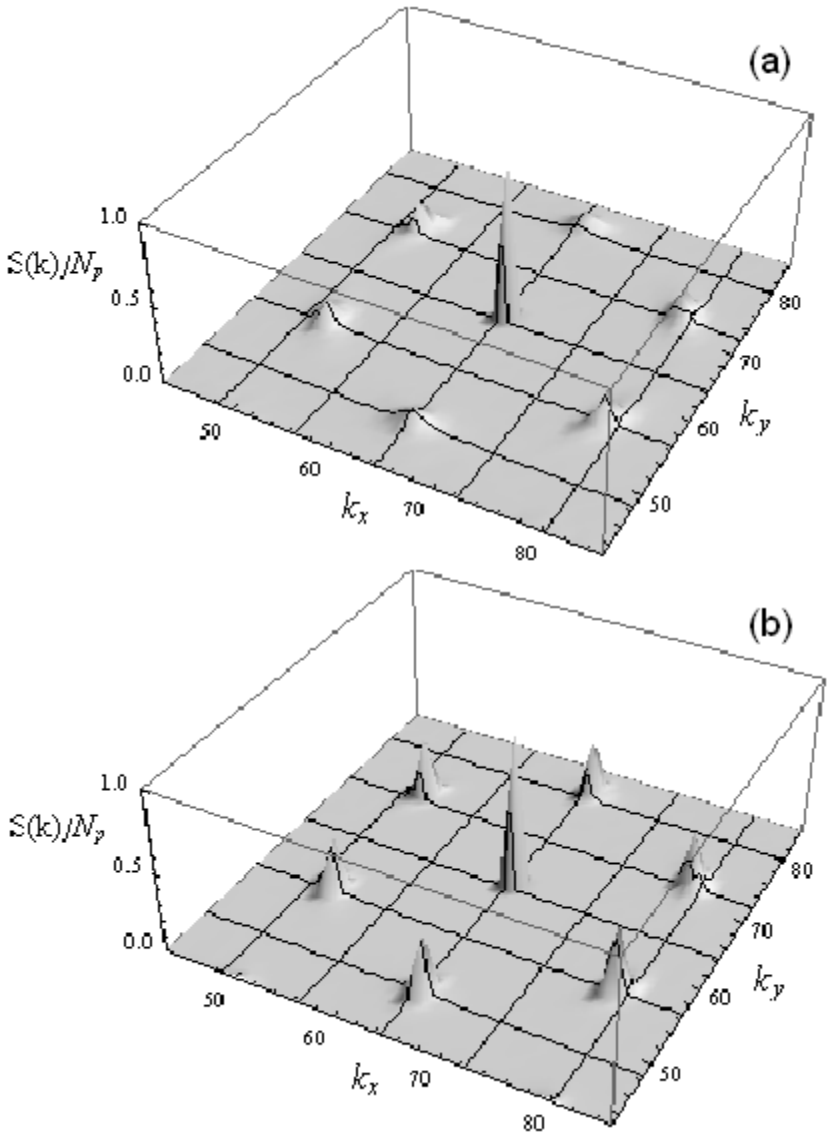
We have studied a two-dimensional PFC model with random pinning. The model provides an effective continuous description of lattice systems in the presence of disordered external pinning centers, allowing for both elastic and plastic deformations. The structural correlations and nonlinear driven response are determined from numerical simulations of the dynamical equations. We find that in the absence of a driving force, the phase-field crystal assumes an amorphous glassy ground state, with short-ranged positional and orientational correlations even in the limit of weak disorder. Under increasing driving force, this pinned amorphous-glass phase evolves first into a moving plastic-flow phase then followed by a moving smectic phase. These results are largely in agreement with previous analytical works [7–9]. An additional new feature is that the transverse response of the moving smectic phase shows a vanishing transverse critical force for increasing system sizes. Finally, we have identified interesting quasi-long range ordered metastable states by evolving initially ordered states in the presence of disorder. The nature of these metastable states are insensitive to the details of disorder and they may be relevant under suitable experimental conditions.

Acknowledgments

E.G. was supported by Fundação de Amparo à Pesquisa do Estado de São Paulo - FAPESP (Grant No. 07/08492-9). K.R.E. acknowledges support from the NSF under Grant No. DMR-0906676. This work was also supported in part by computer facilities from the Centro Nacional de Processamento de Alto Desempenho (CENAPAD-SP and CENAPAD-UFPE).

[1] J.I. Martin, M. Vélez, J. Nogués, and I.K. Schuller, Phys. Rev. Lett. **79**, 1929 (1997).
[2] B.N.J. Persson, Sliding Friction: Physical Principles and Applications (Springer, Heidelberg, 1998).
[3] A. Carlin, L. Bruschi, M. Ferrari, and G. Mistura, Phys. Rev. B **68**, 045420 (2003).
[4] E. Granato and S.C. Ying, Phys. Rev. B **69**, 125403 (2004).
[5] A. Pertsinidis and X.S. Ling, Phys. Rev. Lett. **87**, 098303 (2001).
[6] A. Pertsinidis and X.S. Ling, Phys. Rev. Lett. **100**, 028303 (2008).
[7] T. Giamarchi and P. Le Doussal, Phys. Rev. B **52**, 1242 (1995).
[8] C. Carraro and D.R. Nelson, Phys. Rev. E **56**, 797 (1997).
[9] D. Carpentier and P. Le Doussal, Phys. Rev. Lett. **81**, 1881 (1998).
[10] C. Zeng, P.L. Leath, and D.S. Fisher, Phys. Rev. Lett. **82**, 1935 (1999).
[11] P.L. Doussal and T. Giamarchi, Physica C 331, 233 (2000).
[12] M. Chandran, R.T. Scalettar, and G.T. Zimanyi, Phys.

Rev. B **69**, 024526 (2004).
[13] P. Le Doussal and T. Giamarchi, Phys. Rev. B **57**, 11 356 (1998).
[14] L. Balents, M.C. Marchetti, and L. Radzihovsky, Phys. Rev. B **57**, 7705 (1998).
[15] F. Pardo, F. de la Cruz, P.L. Gammel, E. Bucher, and D.J. Bishop, Nature (London) **396**, 348 (1998).
[16] K. Moon, R.T. Scalettar, and G.T. Zimányi, Phys. Rev. Lett. **77**, 2778 (1996).
[17] C.J. Olson, C. Reichhardt, and F. Nori, Phys. Rev. Lett. **81**, 3757 (1998).
[18] C.J. Olson and C. Reichhardt, Phys. Rev. B **61**, R3811 (2000).
[19] H. Fangohr, P.A.J. de Groot, and S.J. Cox, Phys. Rev. B **63**, 064501 (2001).
[20] C. Reichhardt and C.J. Olson Reichhardt, Phys. Rev. B **76**, 214305 (2007).
[21] J. Lefebvre, M. Hilke, and Z. Altounian, Phys. Rev. B **78**, 134506 (2008).
[22] K.R. Elder, M. Katakowski, M. Haataja, and M. Grant, Phys. Rev. Lett. **88**, 245701 (2002).
[23] K.R. Elder, and M. Grant, Phys. Rev. E **70**, 051605 (2004).
[24] K.R. Elder, N. Provatas, J. Berry, P. Stefanovic, and M. Grant, Phys. Rev. B **75**, 064107 (2007).
[25] C.V. Achim, M. Karttunen, K.R. Elder, E. Granato, T. Ala-Nissila, and S.C. Ying, Phys. Rev. E **74**, 021104 (2006).
[26] J.A.P. Ramos, E. Granato, C.V. Achim, S.C. Ying, K.R. Elder, T. Ala-Nissila, Phys. Rev. E **78**, 031109 (2008).
[27] C.V. Achim, J.A.P. Ramos, M. Karttunen, K.R. Elder, E. Granato, T. Ala-Nissila, and S.C. Ying, Phys. Rev. E **79**, 011606 (2009).
[28] J.A.P. Ramos, E. Granato, S.C. Ying, C.V. Achim, K.R. Elder and T. Ala-Nissila, Phys. Rev. E **81**, 011121(2010).
[29] G. Tegze, G. Bansel, G. I. Tóthb, T. Pusztai, Z. Fan, and L. Gránásy, J. Comput. Phys. **228**, 1612 (2009); B. P. Vollmayr-Lee and Andrew D. Rutenberg, Phys. Rev. E **68**, 066703 (2003); J. Zhu, L.-Q. Chen, J. Shen, and V. Tikare, ibid. **60**, 3564 (1999).
[30] D.R. Nelson and B.I. Halperin, Phys. Rev. B **19**, 2457 (1979).
[31] M.C. Cha and H.A. Fertig, Phys. Rev. Lett. **74**, 4867 (1995).
[32] D.R. Nelson, Phys. Rev. B **27**, 2902 (1983).
[33] S. Herrera-Velarde and H. H. von Grünberg, Soft Matter **5**, 391 (2009).
[34] A.E. Koshelev and V.M. Vinokur, Phys. Rev. Lett. **73**, 3580 (1994).


(a)
1.0
S(k)/N_p
0.5
0.0
50
60
70
80
k_x
50
60
70
80
k_y
(b)
1.0
S(k)/N_p
0.5
0.0
50
60
70
80
k_x
50
60
70
80
k_y